
Imaging of Interventional Therapies in Oncology: Image Guidance, Robotics, and Fusion Systems

17

Helmut Schoellnast and Stephen B. Solomon

Abstract

Image-guided therapies play an increasingly important role in oncology. Several imaging tools for interventional oncology procedures are available or in development which influence the success of the procedures and, therefore, influence the implementation of the procedures into oncologic treatment strategies. In this chapter, a detailed review of medical imaging strategies during an interventional oncology procedure is provided including use of contrast agents for improved tumor visualization, real-time imaging, three-dimensional imaging, fusion of images of different imaging modalities, navigation of devices during interventions, movement of devices by robots, and intraprocedural imaging monitoring. Furthermore, problems of image guidance such as physician access to the patient and radiation exposure are discussed.

In general, the ideal properties of medical imaging during an interventional oncology procedure include (1) sufficient image quality to visualize the tumor targeted as well as the interventional tools and important structures around the tumor; (2) image feedback of the therapy, preferentially in real time, displayed to the interventionalist in the procedure room; and (3) access to the patient by both the interventionalist performing the procedure and other health-care personnel, for example, anesthetist and nurses, during the procedure. In contrast to diagnostic imaging, lower image

quality is an acceptable compromise for real-time imaging for interventional procedures. Patients have already undergone high-quality diagnostic imaging when they are referred to interventional therapies. High-quality diagnostic imaging may require more time and more radiation dose than fast imaging of a restricted region of interest as performed for image guidance of interventions.

Ideally imaging for interventions would provide real-time, three-dimensional displays of information that include the depiction of the target, the interventional tools, and the surrounding anatomy and perhaps for some applications physiologic information indicating areas of contrast enhancement or areas of metabolic activity. The latter is particularly helpful in differentiating viable from necrotic tissue for guiding biopsy or ablation therapy. Although current imaging

H. Schoellnast (✉) • S.B. Solomon
Department of Radiology, Memorial Sloan-Kettering
Cancer Center, New York, NY, USA
e-mail: helmut.schoellnast@gmail.com;
solomons@mskcc.org

systems provide some of these features, none provides all of them. Ultrasound (US) is a real-time, multi-planar technique that provides full access, but the depiction of some tumors is limited especially near bone- and gas-containing structures. In addition, real-time, three-dimensional imaging is limited for interventional applications. CT provides partial access and can be used to guide procedures intermittently, while CT fluoroscopy is near real time, but both have the potential disadvantage of the need for ionizing radiation, which requires one to limit radiation exposure to patients and personnel [1, 2]. CT also is primarily a two-dimensional planar tool; real-time, three-dimensional imaging is not yet fully integrated into interventional CT applications. Open MRI systems have been developed and allow full access to the patient [3], but many MRI-guided interventions today are performed in systems created for diagnostic imaging, and access is limited [4]. Currently, US, CT, and MRI are rarely used with three-dimensional images.

Technical advances of the following areas aim to improve imaging equipment to better meet interventional imaging requirements.

Physician Access to Patient

Physicians must have access to the patient in most interventional oncology procedures to allow real-time guidance as the interventional oncologist places and advances a device. The degree to which the patient is accessible varies from modality to modality. For instance, US and X-ray fluoroscopy provide the most access. During CT-guided procedures, access to patients is more limited due to the gantry surrounding the patient. For example, CT imaging may not be possible during the placement of devices such as long biopsy needles, drainage catheters, and ablation applicators that do not fit in the space between the patient's body surface and the gantry (Fig. 17.1). This is also the major limiting factor to the use of closed-bore MRI systems. MRI allows interventions to be performed for tumors that are visible only with MRI and provides thermal monitoring of ablations [5-10]. MRI offers advantages related to superior soft tissue contrast. However, physician access to the patient in closed-bore, high-, or

Fig. 17.1 Demonstrates how cumbersome current diagnostic imaging equipment may be for performing interventional procedures. The *arrow* shows how the radiofrequency ablation probe cannot fit within the gantry with the patient due to the limited access. The probe needs to be taped to the bore to keep the top-heavy handle from torquing the probe out of the patient



intermediate-field strength MRI systems is a limitation; this has been partially overcome with newer systems [11, 12]. Older “double-doughnut” and open magnets provide access but have lower field strengths (0.5–1.0 T) than recent wider bore magnets (70 cm) with higher field magnets (1.5 T). These systems have been utilized to provide improved access with higher image quality and are facilitating interventional procedures [13, 14]. Many other impediments to MRI-guided intervention, such as the development of MR-compatible instrumentation, have also been solved; some hurdles still remain. Instrument visualization issues still persist whether due to too much artifact or too little conspicuity [15–17]. Noise generated during scanning is potentially harmful to the interventional radiologist, especially with newer high-field (3T) systems [18, 19]. Other challenges still exist such as electrical noise from ablation devices interfering with MR imaging [20]. Similarly to MRI scanners, some newer CT scanners offer 82-cm bores, which provide extended room for interventional procedures. Other solutions make use of semiflexible devices that can bend to accommodate a closed gantry environment [21].

Contrast Agents

Contrast agents are increasingly being applied as interactive tools during intervention. With diagnostic applications, a contrast agent is administered typically once at the beginning of imaging; however, with interventions repeated, smaller contrast doses given intermittently during a procedure may sometimes be helpful. Contrast agents can be used to highlight a target that is not visualized well on non-contrast scans. However, the benefit of most contrast agents in interventional procedures is limited, as they are rapidly cleared and their effects are often transient. Since the use of these agents is dose limited due to renal toxicity, the volume administered during a procedure must be carefully monitored.

New fusion systems that allow overlay of needles on previously acquired enhanced CT imaging may be able to account for the transient nature of contrast enhancement during an intervention.

Contrast agents already play an important role in diagnostic imaging, and new contrast agents are becoming available for all imaging modalities. US contrast agents are comparable to iodine contrast agents concerning tissue enhancement characteristics without subjecting patients to the risk of nephrotoxicity posed by iodinated contrast agents. Contrast agents have been used in US to plan, target, and monitor RF ablations [22–25]. It has been reported that with the routine adoption of contrast-enhanced US, a rate of partial necrosis of 5.9 % was achieved, in comparison with a 16.1 % rate achieved without the real-time management of ablations of hepatocellular and metastatic liver lesions [25]. New, blood-pool, iodinated agents that stay in the vascular space for an extended time and that are hepatocyte selective (such as iodinated triglyceride (ITG)-dual [26]) may be used during CT-guided interventions to delineate blood vessels throughout the procedure or to improve tumor conspicuity in the future [26, 27]. Similar agents are being developed for use in MRI [28]. MRI contrast agents that are aimed at Kupffer cell uptake (superparamagnetic iron oxide particles, SPIO) and agents for the hepatobiliary tree (hepatobiliary-specific MR contrast agents) provide new tools that can be applied to specific cases [29]. Additionally, new thermosensitive MR contrast agents can offer a monitoring tool during thermal ablation by, for example, releasing a contrast agent from a liposome under certain thermal [30–32]. Lastly, advances in molecular imaging are likely to provide improved targeting opportunities that are specific and personalized. For example, new radiotracer-labeled antibodies (such as huA33 and cG250) can specifically target colon cancers or clear cell renal cancers and guide interventions [33, 34].

Real-Time Imaging

CT fluoroscopy, in which real-time CT images are displayed, allows the interventional radiologist to continuously monitor needle placement and has replaced repeated scanning after needle incremental advance as required with standard CT interventions. CT fluoroscopy for interventional procedures was introduced in the early 1990s [35], and it is now widely evaluated for various interventional procedures including the lung, abdominal organs, and the spine [2, 36, 37]. It has been reported that in CT fluoroscopy-guided biopsy of pulmonary lesions with 20-gauge coaxial cutting needles, the biopsy results were nondiagnostic in only 0.6 % of the lesions. The sensitivity and specificity for the diagnosis of malignancy were 94.2 % and 99.1 %, respectively [36].

The downside to CT fluoroscopy is the increased radiation dose and the lack of three-dimensional reconstructions [38]. Attempts to reduce radiation exposure during CT fluoroscopy by lowering the dose applied per section, by implementing angular beam modulation which enables adaption of the tube current to the course of beam and the patient's habitus, and by providing arm extenders have been demonstrated [39-42]. MRI fluoroscopy also provides real-time imaging. Its advantages over CT include the ability to freely select the imaging planes along the needle pathway and the absence of ionizing radiation for the patient [43].

Three-Dimensional Imaging

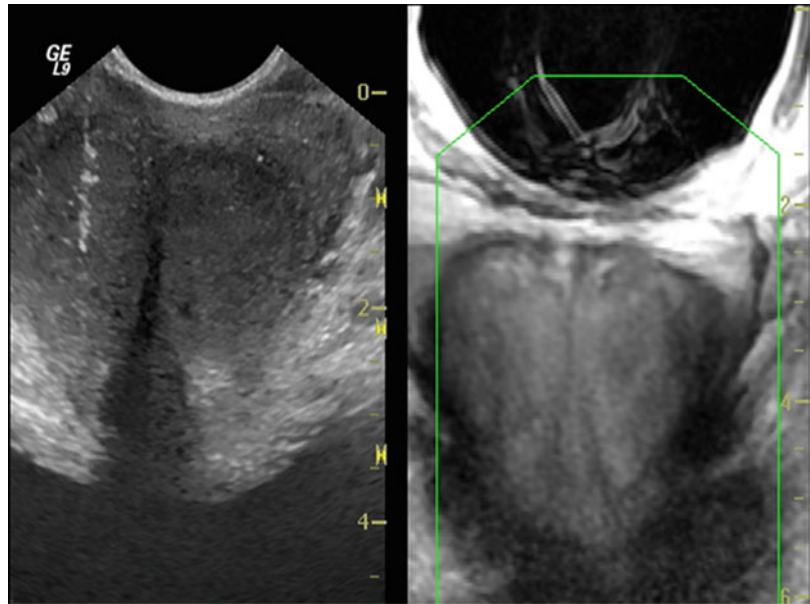
While US, CT, and MRI are still primarily used in two-dimensional, planar mode, efforts are under way to make more use of three-dimensional imaging. For example, in order for a tumor ablation procedure to be successful, the entire tumor volume needs to be treated, without affecting nearby critical structures. Therefore, intraprocedural displays of the tumor in its entire three-dimensional extension and its surroundings would likely improve ablation outcomes.

Preliminary work suggests that three-dimensional imaging is beneficial and assists with applicator placement. One of the limitations to the use of three-dimensional imaging is the time required to create the images and present them to the interventionalist in the procedure suite. The ability to rapidly reconstruct three-dimensional images from these two-dimensional views will further aid image-guided therapy. Rotational flat-panel CT (or cone-beam CT) combine the real-time imaging advantages of fluoroscopy with computed tomography imaging [44-46]. Three-dimensional rotational angiography has been widely applied in neuroradiological interventions. Recent advances in the technology of angiographic equipment have made it feasible to conduct rotational angiography with a large diameter image intensifier allowing coverage of the hepatic vessels [45, 47-51]. It has been reported that 3D rotational flat-panel CT can improve chemoembolization procedure in patients with hepatocellular carcinoma [47, 48, 52]. Software is in evaluation which can be used to segment out the vessels feeding the tumor in 3D angiography images and thereby provide a guide for transcatheter therapy [53]. Providing planar and 3D "CT-like" images with patient access typical of fluoroscopy will allow these machines to take on an even more powerful role in the interventional oncology imaging armamentarium. Although visualization of dense structures such as bone and contrast-filled vessels on these systems is adequate, challenges still remain in soft tissue resolution. As this relatively new technology improves, the need for helical CT to guide many interventional procedures may be reduced.

Image Registration and Fusion

Image registration is defined as aligning two imaging data sets spatially to each other. Fusion is defined as overlaying them and visualizing them as one image. Image fusion may be performed to combine metabolic imaging with anatomical imaging (e.g., fluorodeoxyglucose (FDG) PET with CT) or to combine real-time

Fig. 17.2 Demonstrates image registration to guide prostate biopsy. The *left* image shows time transrectal ultrasound of the prostate; the *right* image shows prior acquired endorectal MRI which is aligned to the real-time ultrasound image on the *left*



anatomic imaging with non-real-time imaging of a second anatomic imaging modality (e.g., US with CT). While metabolic imaging such as fluorodeoxyglucose (FDG) PET has had a major impact on detecting and staging cancers, its role in interventional radiology has been limited because of the lack of sufficient anatomic detail required for image guidance. While combined PET/CT, SPECT/CT, or even PET/MR systems exist, interventions usually occur in CT or MR systems independent of PET or SPECT equipment. To best utilize these PET images for imaging guidance, they must be fused with the CT images. Fusion, or overlay, of PET images with CT or MR images allows the utilization of both the anatomic detail of CT or MRI and the physiologic information of PET [54-56]. US images also may be fused with CT images obtained pre-procedurally to gain the real-time, nonionizing radiation information of US with the anatomic detail of a contrast-enhanced CT [57, 58]. This potential benefit in combining these modalities may be used for image-guided interventions. US systems in which a previously recorded CT or MRI examination is shown simultaneously with real-time US are commercially available from different vendors. An existing CT or MRI data set is loaded into the system, and the CT or MRI

images are reformatted in a projection to fit the live sonography images. The advantage of this method is that structures that are difficult to outline on US are shown on the CT or MRI images, and yet real-time ultrasound imaging can still be utilized. In a phantom study using a fusion navigating system [59], a rate of success in obtaining biopsies from US invisible spheres of 72 % has been reported for the first needle pass and of 88 % within two needle passes. In a clinical study [60] in patients with prostate cancer, transrectal US images were registered with pre-procedural-acquired endorectal MRI for biopsy guidance. The authors concluded that the fusion of real-time transrectal US and prior MR images of the prostate (dynamic contrast-enhanced maps, or T2-weighted or MR spectroscopy images) is feasible and enables MRI-guided interventions outside of the MRI suite [60] (Fig. 17.2).

Also, MR images may be fused with intraprocedural, unenhanced CT to provide better depiction of tumor margins for targeting as MRI features higher soft tissue resolution than CT [61]. Fusion has also been used to overlay fluoroscopy with cone-beam CT, CT, or MRI to provide additional guidance during embolization procedures (Fig. 17.3) [62]. Multimodality image fusion may aid interventional radiologists substantially, but



Fig. 17.3 Shows a fused image of a contrast-enhanced cone-beam CT and a live 2D-fluoroscopy image. The cone-beam CT has been segmented to demonstrate the enhanced hepatic arterial tree. It is registered with the fluoroscopy image automatically by maintaining the same table for both imaging studies

patient breathing, patient positioning, organ shift, and even procedure-/instrument-related motion challenge image registration and fusion [63, 64]. The challenge of multimodality fusion is simplified when both imaging data sets are obtained on the same patient bed through the use of multimodality imaging suites. These hybrids, combination suites with CT and fluoroscopy or MR and fluoroscopy, are being used and offer easier image registration since patients remain on the same table and in the same position for both imaging studies. However, these hybrid units are costly limiting their practicality.

Navigation

The integration of position sensors with interventional devices such as needles and ablation applicators allows them to be tracked real time with imaging obtained during a procedure. Tracking displays the needle or applicator location in relation to the pre-procedural-acquired images. Tracking can be accomplished with mechanical

arms, with optical systems, or with electromagnetic systems. Electromagnetic tracking allows tracking of internal medical devices, whereas optical tracking requires direct line of sight, which is less useful for image-guided therapy which may utilize flexible needles [65]. Miniaturization of electromagnetic sensors and needles with sensors integrated inside the tip has enabled spatial tracking of needles. Internalized needle-tip sensors actually track and follow the motion of the needle itself and do not rely on the estimation of needle position on the basis of external needle hub position. This can correct for needle bending, organ motion, and respiration [66] (Fig. 17.4).

When used with multimodality image fusion, the coordinates of the device's tip can be superimposed on previously acquired images or on real-time imaging. When a pre-procedural CT scan is fused with real-time US, the position of the device can be tracked in real time such that its position is known in relationship to anatomy displayed both on CT and US. It may also allow the physiologic images such as PET to be incorporated into an intervention. Additionally, device tracking may allow out-of-plane trajectory imaging such as directing a needle to the dome of the liver without transgressing pleura. Navigation has even been reported on cone-beam CT images to further enable procedures in fluoroscopy rooms [67]. However, all these navigation tools face the same image registration engineering challenges that image fusion does [65, 68-72].

Robotics

According to the Robotic Institute of America (1979), a robot is “a reprogrammable, multifunctional manipulator designed to move materials, parts, tools, or other specialized devices through various programmed motions for the performance of a variety of tasks.” Robotics have been applied to several areas of medicine [73]. Since modern medical imaging is digital and robots function in a digital world, it makes sense that robotics can be applied to interventional oncology. Robots in interventional oncology, currently, have two potential roles. First, they may

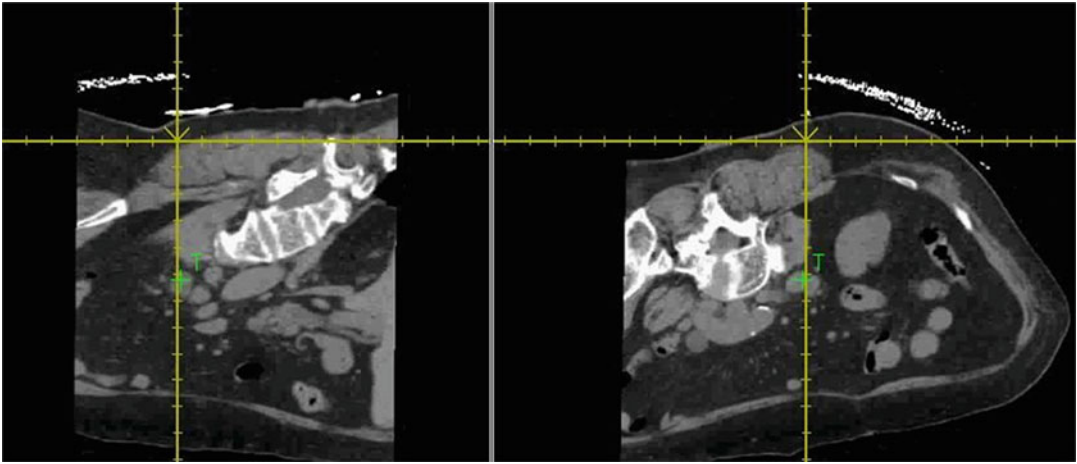


Fig. 17.4 Shows two images from a navigation study where an electromagnetic system was used to guide a needle to a retroperitoneal lymph node (*arrow*). The needle tip is at the skin prior to entry with the *arrow*

showing the direction to the lymph node (*T target*). *Left* image shows sagittal-oblique view; *right* image shows transverse-oblique view

act as “arm extenders” during fluoroscopy and CT-guided interventions and thereby limit physician radiation exposure. Second, robots may improve the accuracy of device placement [64, 74, 75]. Using integrated software systems, the coordinates of targets can be chosen, and then the robot can deliver a device to the prescribed location. Robotic precision may be helpful to ensure overlapping ablations and ensure safe probe separation. Robots have been applied to CT, MRI, fluoroscopy, and even US-guided procedures [76–78]. Accurate targeting, however, requires that the image used for planning is registered with the patient and accounts for patient motion. These, therefore, are the same engineering challenges that are faced with navigation and fusion enhancements.

While medical robots have been applied in many fields such as neurosurgery, orthopedics, and urology, they are not the standard of care in any field. Studies on phantoms and animals as well as clinical trials have been performed using fluoroscopy, US, CT, and MRI as imaging modality. The AcuBot robot has been developed in the URobotics Laboratory at Johns Hopkins Medical Institutions (Baltimore, USA) (Fig. 17.5) [64]. Four clinical cases of CT-guided kidney and spine biopsy and radiofrequency ablation and a nephrostomy tube placement were successfully

performed with no complications [79]. Another study showed that the use of the robot in CT-guided core biopsies and radiofrequency ablations reduced radiation exposure for the patient and medical personnel [75]. The B-Rob system which has been developed by ARC Seibersdorf Research (Seibersdorf, Austria) enables CT-guided and US-guided biopsies. The first in vitro trials of the system show a high accuracy (0.66 ± 0.27 mm) in image-guided positioning of a biopsy, and a risk analysis of the complete system did not find any major risks [64, 80]. A series of quantitative evaluation studies is currently in process at different research centers. The robotic instrument-guiding system INNOMOTION (Innomedic, Herxheim and FZK Karlsruhe, Germany) has been developed to provide MRI compatibility. The system has shown a precision of the insertion site in the axial plane was ± 2 mm (0.5–3 mm). The angular deviation in the transverse plane of the cannulae was $\pm 1^\circ$ (0.5° – 3°) [64]. The MrBot robot has been developed at URobotics Laboratory at Johns Hopkins Medical Institutions (Baltimore, USA) for fully automated image-guided transperineal access of the prostate gland, and a recent robot developed by this research group is under way for transrectal access. In the future, this robot may enable better targeted prostate image-guided therapies.

Fig. 17.5 Depicts the AcuBot which is a CT robot for needle placement. The robot is mounted to the CT table and can be registered with the CT image



Intraprocedural Monitoring

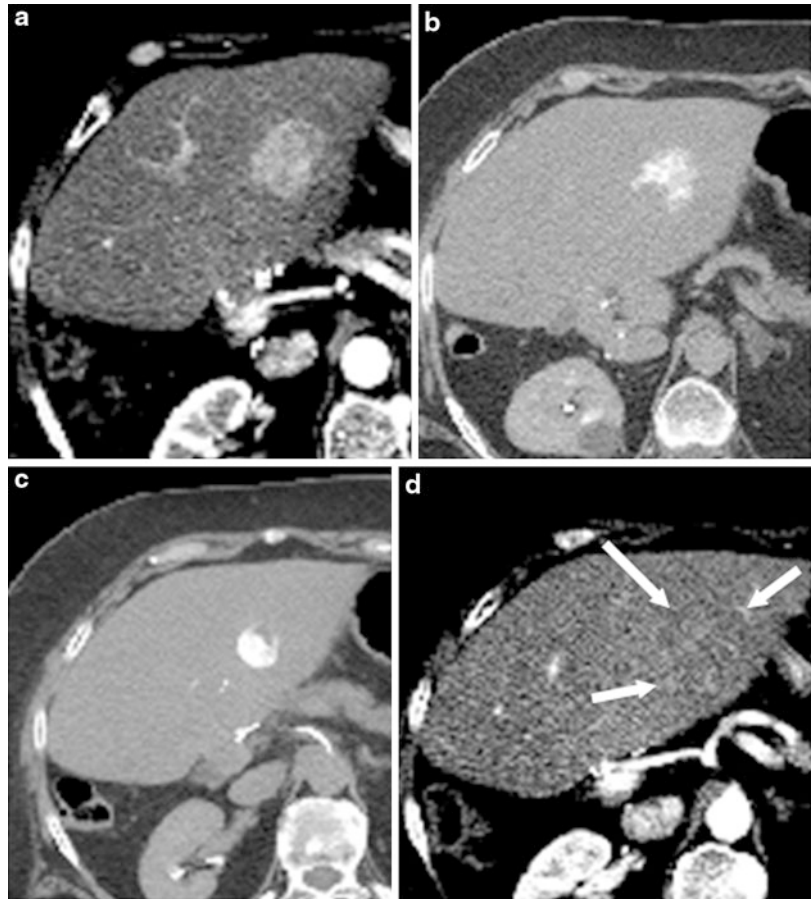
Evaluation of treatment success during and immediately after the procedure is an important challenge in most interventional oncologic therapies. Ideally there would be some clear endpoint for therapy completion. Imaging is a preferable potential solution in this matter due to its noninvasive measure of completeness. The term monitoring can be defined as imaging that is used during the procedure and immediately after the procedure that visualizes changes that result from the procedure. The goal of monitoring is to not only determine if the treatment is complete but also display the surrounding critical structures that should not be affected more than is necessary to complete the treatment effectively and safely.

Several imaging modalities have been used to assess completeness of therapy. These primarily revolve around measures of blood flow. Angiography after (chemo-)embolization of hypervascular tumors can show hemostasis and a completely embolized tumor bed. Lipiodol or contrast laden-embolic material uptake may be used to visualize progress during chemoembolization

and bland embolization procedures, respectively (Fig. 17.6). This may be especially well visualized on 3D rotational flat-panel CT. Recently combined MR–X-ray systems have allowed intraprocedural transcatheter intra-arterial perfusion MRI to be performed during hepatic artery embolization to permit intraprocedural perfusion changes and monitoring [81].

With US, Doppler flow and contrast agents have been used to assess blood flow and determine when a tumor no longer has a viable blood supply after an ablation [25, 82]. US may also be used without contrast to monitor the effects of an ablation based on changes in echogenicity. During RF ablation, increased echogenicity can be seen in the ablation zone which diameter correlates with the diameter of necrosis [83]. However, the solitary diameter of the echogenic response may be greater than the smallest diameter and less than the largest diameter of the area of tissue necrosis. Therefore, the echogenic response associated with radiofrequency ablation should be viewed only as a rough approximation of the area of induced tissue necrosis; the final assessment of the adequacy of ablation should be deferred to an alternative imaging technique [83]. Furthermore, this increased echogenicity may

Fig. 17.6 (a–d) Shows the importance of intraprocedural monitoring to determine completeness of an image-guided bland embolization procedure. (a) Pre-procedure contrast-enhanced CT indicating an enhancing hepatocellular carcinoma, (b) mid-procedure non-contrast CT image with contrast laden particles showing a partially embolized tumor, (c) mid-procedure CT image with contrast laden particles filling the rest of the tumor, and (d) contrast-enhanced CT after the embolization procedure without enhancement of the tumor. Fusing these mid-procedure images (b–c) can help guide the interventionalist to a complete treatment



obscure imaging during the procedure and hinder probe replacement. During cryotherapy, an echogenic mass-like structure with distal acoustic shadowing representing the ice ball formation may be noted.

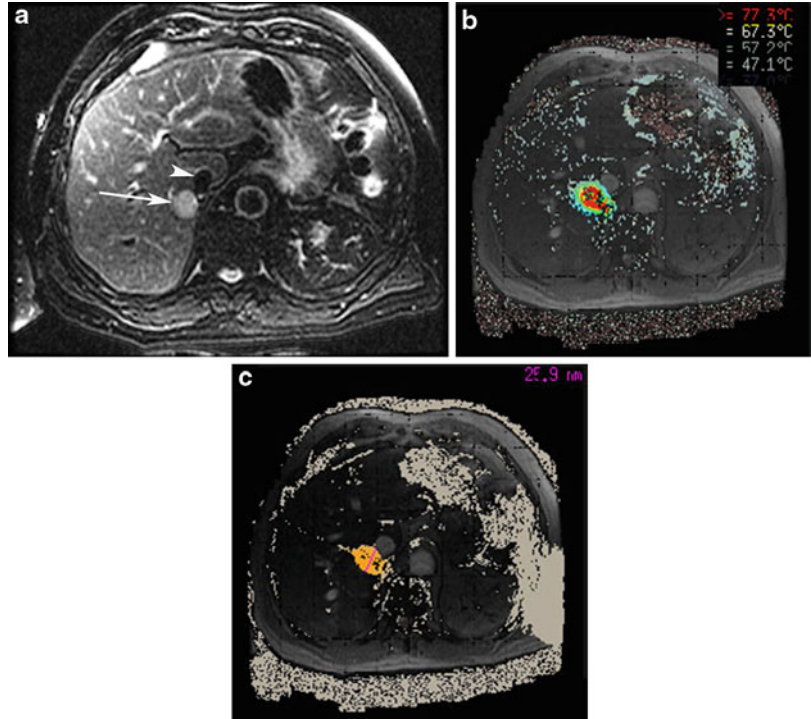
Like US, CT and MRI can also provide intraprocedural imaging feedback during a therapy. Contrast agents may be used in CT and MRI to assess vascularity of the treatment zone. Unlike US, the cryotherapy ice ball can be viewed in its entirety using both CT and MRI [10, 84]. Intraprocedural T2-weighted fast spin-echo images can be obtained every 2–3 min, which allow real-time ice ball monitoring and accurate prediction of the region of cryo-necrosis [85]. During ethanol-ablation procedures, CT low attenuation associated with percutaneous ethanol injection can guide procedure termination [86–88]. Conceivably nuclear medicine agents in

the future, such as $[^{15}\text{O}]\text{-H}_2\text{O}$, might be useful to measure tumor viability during a procedure and guide therapy completion. The short, 2-min half-life of $[^{15}\text{O}]$ makes it possible to perform repeated PET imaging at 20-min intervals at multiple time points before and after image-guided therapy. $[^{15}\text{O}]\text{-water}$ PET demonstrates the ablated tumor region, whereas the unablated tumor continued to show high $[^{15}\text{O}]\text{-water}$ accumulation [89].

More recently imaging has also been used to measure tissue temperatures; these techniques can help monitor thermal ablations and assure that the tumor is completely treated and critical structures not harmed [90]. Since maintaining temperatures of $\sim 54^\circ\text{C}$ or higher for longer than one second is believed to cause cell death, measuring temperature with MRI can provide a quantitative noninvasive method of evaluating

Fig. 17.7 (a–c)

Demonstrates MRI-guided laser ablation of solitary liver metastases. (a) Pretreatment T2-weighted fat-suppressed imaging reveals the hyperintense lesion (*arrow*) adjacent to the inferior vena cava (*arrowhead*). (b) MR thermometry during ablation was used to ensure adequate heating and avoidance of critical structures. Colors represent different levels of temperature. (c) Image after ablation shows tissue where the temperature was above 60 °C in orange to estimate the ablation area



the completeness of a thermal ablation. Understanding the thermal dose delivered may even facilitate some selectivity of tissue destruction since different tissues have different thresholds for death [91]. While a number of temperature-sensitive MR techniques, based on the relaxation time $T(1)$, the diffusion coefficient (D), or proton resonance frequency (PRF) of tissue water, have also been used, proton resonance frequency changes are probably most commonly used clinically [92]. The excellent linearity of the temperature dependency of the proton resonance frequency (PRF) and its near independence with respect to tissue type make the PRF-based methods the preferred choice for many applications. A standard deviation of less than 1 °C, for a temporal resolution below 1 s and a spatial resolution of approximately 2 mm, is feasible for immobile tissues [93]. MR thermometry has been primarily developed for use with high-intensity focused US [31, 94] but has also been applied to other ablative agents, such as radiofrequency, laser, microwave, and hot saline [95–101] (Fig. 17.7). Limitations of MR thermometry still exist due to motion, magnetic

field inhomogeneities created by ablation tools or fatty environments, and those due to the limited temporal resolution of the technique.

Although less developed to date and not yet in clinical practice, both CT and US have been suggested as noninvasive modalities to measure tissue temperatures. CT attenuation and sound velocity have both been shown to correlate with temperature [102, 103].

Radiation Exposure

Many procedures are best done using CT or X-ray fluoroscopy as the guidance modality. Their inherent limitation is the radiation exposure to physician and patient. For example, excessive radiation exposure to physician and patient can occur during CT fluoroscopy because of continuous exposure at a single anatomic location. On the other hand, excessively low radiation doses lead to inferior image quality and result in interference with IR procedures. In addition to wearing lead aprons and other protective garb, physician exposure can be diminished further during CT

fluoroscopy-guided procedures by placing a lead shield on the patient just below the imaging plane to reduce scatter radiation and by using “arm extenders” such as robots described above [2]. Modifications to the imaging protocol can also be employed to limit radiation exposure. Lowering tube current and tube potential and reducing the time the beam is on during a rotation reduce radiation exposure directly. On the basis of the As Low As Reasonably Achievable (ALARA) principle, one should use the CT fluoroscopic scan parameters which provide acceptable image quality at the lowest possible radiation exposure. For example, acceptable image quality can be achieved with a tube voltage of 135 kV and a tube current of 10 mA (1.48 mGy/s) for CT fluoroscopy in lung interventional procedures [40]. Adapting the tube load to the patient’s size and shape with the aim to keep image noise constant throughout the entire study has also proved to lower the radiation dose to the minimum required. Both in-plane (XY-axis) and longitudinal (Z-axis) dose modulation are embedded in 64-slice CTs [39]. In addition, the use of navigation software and fusion imaging may potentially reduce the time required to do the procedure, thereby indirectly reducing radiation exposure [104, 105].

The dose for rotational flat-panel CT is similar to those used for corresponding MDCT scans with comparable slice thickness [106]. The effect of rotational flat-panel CT on overall patient dose remains to be seen. On the one hand, judicious use of in-suite rotational flat-panel CT may actually result in a decrease in patient dose by providing critical diagnostic information that obviates the need for excessive fluoroscopy. Alternatively, the simple availability of this technique may lead to overuse and increased patient radiation [107].

Conclusion

Imaging plays a critical role in interventional oncology procedures. It is needed for guidance and monitoring. As these tools are adapted from diagnostic roles to interventional ones, they require modification. Some of these

modifications have begun to occur, while others are still in their infancy. Image fusion and robotics, for example, represent two areas of potential applicability to interventional oncology procedures. As imaging evolves to meet the needs of interventional oncology, the interventionalist will be enabled to accomplish even more with image-guided, less invasive techniques.

References

1. Nawfel RD, Judy PF, Silverman SG, Hooton S, Tuncali K, Adams DF. Patient and personnel exposure during CT fluoroscopy-guided interventional procedures. *Radiology*. 2000;216:180–4.
2. Silverman SG, Tuncali K, Adams DF, Nawfel RD, Zou KH, Judy PF. CT fluoroscopy-guided abdominal interventions: techniques, results, and radiation exposure. *Radiology*. 1999;212:673–81.
3. Lewin JS, Nour SG, Connell CF, et al. Phase II clinical trial of interactive MR imaging-guided interstitial radiofrequency thermal ablation of primary kidney tumors: initial experience. *Radiology*. 2004;232:835–45.
4. Tatli S, Morrison PR, Tuncali K, Silverman SG. Interventional MRI for oncologic applications. *Tech Vasc Interv Radiol*. 2007;10:159–70.
5. Gedroyc WM. Magnetic resonance guidance of thermal ablation. *Top Magn Reson Imaging*. 2005; 16:339–53.
6. Mougnot C, Quesson B, de Senneville BD, et al. Three-dimensional spatial and temporal temperature control with MR thermometry-guided focused ultrasound (MRgHIFU). *Magn Reson Med*. 2009;61:603–14.
7. Pech M, Wieners G, Freund T, et al. MR-guided interstitial laser thermotherapy of colorectal liver metastases: efficiency, safety and patient survival. *Eur J Med Res*. 2007;12:161–8.
8. Puls R, Langner S, Rosenberg C, et al. Laser ablation of liver metastases from colorectal cancer with MR thermometry: 5-year survival. *J Vasc Interv Radiol*. 2009;20:225–34.
9. Silverman SG, Tuncali K, Adams DF, et al. MR imaging-guided percutaneous cryotherapy of liver tumors: initial experience. *Radiology*. 2000; 217:657–64.
10. Silverman SG, Tuncali K, Morrison PR. MR Imaging-guided percutaneous tumor ablation. *Acad Radiol*. 2005;12:1100–9.
11. Boss A, Clasen S, Kuczyk M, et al. Magnetic resonance-guided percutaneous radiofrequency ablation of renal cell carcinomas: a pilot clinical study. *Invest Radiol*. 2005;40:583–90.
12. Morrison PR, Silverman SG, Tuncali K, Tatli S. MRI-guided cryotherapy. *J Magn Reson Imaging*. 2008;27:410–20.

13. Fritz J, Clasen S, Boss A, et al. Real-time MR fluoroscopy-navigated lumbar facet joint injections: feasibility and technical properties. *Eur Radiol.* 2008;18:1513–18.
14. Stattaus J, Maderwald S, Forsting M, Barkhausen J, Ladd ME. MR-guided core biopsy with MR fluoroscopy using a short, wide-bore 1.5-Tesla scanner: feasibility and initial results. *J Magn Reson Imaging.* 2008;27:1181–7.
15. Smits HF, Bos C, van der Weide R, Bakker CJ. Interventional MR: vascular applications. *Eur Radiol.* 1999;9:1488–95.
16. Thomas C, Springer F, Röthke M, et al. In vitro assessment of needle artifacts with an interactive three-dimensional MR fluoroscopy system. *J Vasc Interv Radiol.* 2010;21:375–80.
17. Weiss CR, Nour SG, Lewin JS. MR-guided biopsy: a review of current techniques and applications. *J Magn Reson Imaging.* 2008;27:311–25.
18. Moelker A, Maas RAJJ, Lethimonnier F, Pattynama PMT. Interventional MR imaging at 1.5 T: quantification of sound exposure. *Radiology.* 2002;224:889–95.
19. Moelker A, Wielopolski PA, Pattynama PMT. Relationship between magnetic field strength and magnetic-resonance-related acoustic noise levels. *Magn Reson Mater Phys Biol Med.* 2003;16:52–5.
20. Nour SG, Lewin JS. Radiofrequency thermal ablation: the role of MR imaging in guiding and monitoring tumor therapy. *Magn Reson Imaging Clin N Am.* 2005;13:561–81.
21. Gaffke G, Gebauer B, Knollmann FD, et al. Use of semiflexible applicators for radiofrequency ablation of liver tumors. *Cardiovasc Intervent Radiol.* 2006;29:270–5.
22. Chen MH, Yang W, Yan K, et al. The role of contrast-enhanced ultrasound in planning treatment protocols for hepatocellular carcinoma before radiofrequency ablation. *Clin Radiol.* 2007;62:752–60.
23. Liu JB, Wansaicheong G, Merton DA, et al. Canine prostate: contrast-enhanced US-guided radiofrequency ablation with urethral and neurovascular cooling—initial experience. *Radiology.* 2008;247:717–25.
24. Numata K, Isozaki T, Ozawa Y, et al. Percutaneous ablation therapy guided by contrast-enhanced sonography for patients with hepatocellular carcinoma. *AJR Am J Roentgenol.* 2003;180:143–9.
25. Solbiati L, Ierace T, Tonolini M, Cova L. Guidance and monitoring of radiofrequency liver tumor ablation with contrast-enhanced ultrasound. *Eur J Radiol.* 2004;51(Suppl):S19–23.
26. Weichert JP, Lee FT, Chosy SG, et al. Combined hepatocyte-selective and blood-pool contrast agents for the CT detection of experimental liver tumors in rabbits. *Radiology.* 2000;216:865–71.
27. Fu Y, Nitecki DE, Maltby D, et al. Dendritic iodinated contrast agents with PEG-cores for CT imaging: synthesis and preliminary characterization. *Bioconjug Chem.* 2006;17:1043–56.
28. Burtea C, Laurent S, Vander Elst L, Muller RN. Contrast agents: magnetic resonance. In: Semmler W, Schwaiger M, editors. *Molecular imaging I: handbook of experimental pharmacology.* Berlin/Heidelberg: Springer; 2008. p. 135–65.
29. Bartolozzi C, Crocetti L, Lencioni R, Cioni D, Della Pina C, Campani D. Biliary and reticuloendothelial impairment in hepatocarcinogenesis: the diagnostic role of tissue-specific MR contrast media. *Eur Radiol.* 2007;17:2519–30.
30. Lindner LH, Reintl HM, Schlemmer M, Stahl R, Peller M. Paramagnetic thermosensitive liposomes for MR-thermometry. *Int J Hyperthermia.* 2005;21: 575–88.
31. McDannold N, Tempany CM, Fennessy FM, et al. Uterine leiomyomas: MR imaging-based thermometry and thermal dosimetry during focused ultrasound thermal ablation. *Radiology.* 2006;240: 263–72.
32. Needham D, Dewhirst MW. The development and testing of a new temperature-sensitive drug delivery system for the treatment of solid tumors. *Adv Drug Deliv Rev.* 2001;53:285–305.
33. Strong VE, Humm J, Russo P, et al. A novel method to localize antibody-targeted cancer deposits intraoperatively using handheld PET beta and gamma probes. *Surg Endosc Inter Tech.* 2008;22:386–91.
34. Wendler T, Traub J, Ziegler SI, Navab N. Navigated three dimensional beta probe for optimal cancer resection. *Med Image Comput Comput Assist Interv.* 2006;9:561–9.
35. Katada K, Kato R, Anno H, et al. Guidance with real-time CT fluoroscopy: early clinical experience. *Radiology.* 1996;200:851–6.
36. Hiraki T, Mimura H, Gobara H, et al. CT Fluoroscopy-guided biopsy of 1,000 pulmonary lesions performed with 20-gauge coaxial cutting needles. *Chest.* 2009;136:1612–17.
37. Trumm CG, Jakobs TF, Zech CJ, Helmberger TK, Reiser MF, Hoffmann R-T. CT Fluoroscopy-guided percutaneous vertebroplasty for the treatment of osteolytic breast cancer metastases: results in 62 sessions with 86 vertebrae treated. *J Vasc Interv Radiol.* 2008;19:1596–606.
38. de Mey J, Op de Beeck B, Meysman M, et al. Real time CT-fluoroscopy: diagnostic and therapeutic applications. *Eur J Radiol.* 2000;34:32–40.
39. Hohl C, Suess C, Wildberger JE, et al. Dose reduction during CT fluoroscopy: phantom study of angular beam modulation. *Radiology.* 2008;246:519–25.
40. Yamato Y, Yamakado K, Takaki H, et al. Optimal scan parameters for CT fluoroscopy in lung interventional radiologic procedures: relationship between radiation dose and image quality. *Radiology.* 2010;255:233–41.
41. Neeman Z, Dromi SA, Sarin S, Wood BJ. CT fluoroscopy shielding: decreases in scattered radiation for the patient and operator. *J Vasc Interv Radiol.* 2006;17:1999–2004.

42. Irie T, Kajitani M, Itai Y. CT fluoroscopy-guided intervention: marked reduction of scattered radiation dose to the physician's hand by use of a lead plate and an improved I-I device. *J Vasc Interv Radiol.* 2001;12:1417-21.
43. Yutzy SR, Duerk JL. Pulse sequences and system interfaces for interventional and real-time MRI. *J Magn Reson Imaging.* 2008;27:267-75.
44. Beldi G, Styner M, Schindera S, Inderbitzin D, Candinas D. Intraoperative three-dimensional fluoroscopic cholangiography. *Hepatogastroenterology.* 2006;53:157-9.
45. Liapi E, Hong K, Georgiades CS, Geschwind JF. Three-dimensional rotational angiography: introduction of an adjunctive tool for successful transarterial chemoembolization. *J Vasc Interv Radiol.* 2005;16:1241-5.
46. Wallace MJ. C-arm computed tomography for guiding hepatic vascular interventions. *Tech Vasc Interv Radiol.* 2007;10:79-86.
47. Iwazawa J, Ohue S, Mitani T, et al. Identifying feeding arteries during TACE of hepatic tumors: comparison of C-arm CT and digital subtraction angiography. *AJR Am J Roentgenol.* 2009;192:1057-63.
48. Kakeda S, Korogi Y, Hatakeyama Y, et al. The usefulness of three-dimensional angiography with a flat panel detector of direct conversion type in a transcatheter arterial chemoembolization procedure for hepatocellular carcinoma: initial experience. *Cardiovasc Intervent Radiol.* 2008;31:281-8.
49. Kakeda S, Korogi Y, Ohnari N, et al. Usefulness of cone-beam volume CT with flat panel detectors in conjunction with catheter angiography for transcatheter arterial embolization. *J Vasc Interv Radiol.* 2007;18:1508-16.
50. Kim HC, Chung JW, Park JH, et al. Transcatheter arterial chemoembolization for hepatocellular carcinoma: prospective assessment of the right inferior phrenic artery with C-arm CT. *J Vasc Interv Radiol.* 2009;20:888-95.
51. Matsui O, Kadoya M, Yoshikawa J, et al. Small hepatocellular carcinoma: treatment with subsegmental transcatheter arterial embolization. *Radiology.* 1993;188:79-83.
52. Tanigawa N, Komemushi A, Kojima H, Kariya S, Sawada S. Three-dimensional angiography using rotational digital subtraction angiography: usefulness in transarterial embolization of hepatic tumors. *Acta Radiol.* 2004;45:602-7.
53. Solomon S, Thornton R, Deschamps F, et al. A treatment planning system for transcatheter hepatic therapies: pilot study. *J Interv Oncol.* 2008;1:12-8.
54. Heron DE, Smith RP, Andrade RS. Advances in image-guided radiation therapy – the role of PET-CT. *Medical Dosimetry.* 2006;31:3-11.
55. Veit P, Kuehle C, Beyer T, Kuehl H, Bockisch A, Antoch G. Accuracy of combined PET/CT in image-guided interventions of liver lesions: an ex-vivo study. *World J Gastroenterol.* 2006;12:2388-93.
56. Yap JT, Carney JPJ, Hall NC, Townsend DW. Image-guided cancer therapy using PET/CT. *Cancer J.* 2004;10:221-33.
57. Crocetti L, Lencioni R, DeBenedictis S, See TC, Della Pina C, Bartolozzi C. Targeting liver lesions for radiofrequency ablation – an experimental feasibility study using a CT-US fusion imaging system. *Invest Radiol.* 2008;43:33-9.
58. Wein W, Roper B, Navab N. Automatic registration and fusion of ultrasound with CT for radiotherapy. *Med Image Comput Assist Interv.* 2005;8(Pt 2):303-11.
59. Ewertsen C, Grossjohann HS, Nielsen KR, Torp-Pedersen S, Nielsen MB. Biopsy guided by real-time sonography fused with MRI: a phantom study. *Am J Roentgenol.* 2008;190:1671-4.
60. Singh AK, Kruecker J, Xu S, et al. Initial clinical experience with real-time transrectal ultrasonography-magnetic resonance imaging fusion-guided prostate biopsy. *BJU Int.* 2008;101:841-5.
61. Archip N, Tatli S, Morrison P, Jolesz F, Warfield SK, Silverman S. Non-rigid registration of pre-procedural MR images with intra-procedural unenhanced CT images for improved targeting of tumors during liver radiofrequency ablations. *Med Image Comput Assist Interv.* 2007;10:969-77.
62. Gutierrez LF, Silva R, Ozturk C, et al. Technology preview: X-ray fused with magnetic resonance during invasive cardiovascular procedures. *Catheter Cardiovasc Interv.* 2007;70:773-82.
63. Solomon SB. Incorporating CT, MR imaging, and positron emission tomography into minimally invasive therapies. *J Vasc Interv Radiol.* 2005;16:445-7.
64. Cleary K, Melzer A, Watson V, Kronreif G, Stoianovici D. Interventional robotic systems: applications and technology state-of-the art. *Minim Invasive Ther Allied Technol.* 2006;15:101-13.
65. Wood B, Locklin J, Viswanathan A, et al. Technologies for guidance of radiofrequency ablation in the multimodality interventional suite of the future. *J Vasc Interv Radiol.* 2007;18:9-24.
66. Kruecker J, Xu S, Glossop N, et al. Electromagnetic tracking for thermal ablation and biopsy guidance: clinical evaluation of spatial accuracy. *J Vasc Interv Radiol.* 2007;18:1141-50.
67. Meyer BC, Peter O, Nagel M, et al. Electromagnetic field-based navigation for percutaneous punctures on C-arm CT: experimental evaluation and clinical application. *Eur Radiol.* 2008;18:2855-64.
68. Borgert J, Kruger S, Timinger H, et al. Respiratory motion compensation with tracked internal and external sensors during CT-guided procedures. *Comput Aided Surg.* 2006;11:119-25.
69. Mogami T, Dohi M, Harada J. A new image navigation system for MR-guided cryosurgery. *Magn Reson Med Sci.* 2002;1:191-7.

70. Peters TM. Image-guidance for surgical procedures. *Phys Med Biol.* 2006;51:R505–40.
71. Solomon SB. Interactive images in the operating room. *J Endourol.* 1999;13:471–5.
72. Zhang H, Banovac F, Lin R, et al. Electromagnetic tracking for abdominal interventions in computer aided surgery. *Comput Aided Surg.* 2006;11:127–36.
73. Marohn MR, Hanly EJ. Twenty-first century surgery using twenty-first century technology: surgical robotics. *Curr Surg.* 2004;61:466–73.
74. Hempel E, Fischer H, Gumb L, et al. An MRI-compatible surgical robot for precise radiological interventions. *Comput Aided Surg.* 2003;8:180–91.
75. Solomon SB, Patriciu A, Bohlman ME, Kavoussi LR, Stoianovici D. Robotically driven interventions: a method of using CT fluoroscopy without radiation exposure to the physician. *Radiology.* 2002;225:277–82.
76. Boctor EM, Choti MA, Burdette EC, Webster III RJ. Three-dimensional ultrasound-guided robotic needle placement: an experimental evaluation. *Int J Med Robot.* 2008;4:180–91.
77. DiMaio SP, Pieper S, Chinzei K, et al. Robot-assisted needle placement in open MRI: system architecture, integration and validation. *Comput Aided Surg.* 2007;12:15–24.
78. Stoianovici D. Multi-imager compatible actuation principles in surgical robotics. *Int J Med Robot.* 2005;1:86–100.
79. Patriciu A, Solomon S, Kavoussi LR, Stoianovici D. Robotic kidney and spine percutaneous procedures using a new laser-based CT registration method. In: Niessen W, Viergever MA, editors. *Medical image computing and computer-assisted intervention, Lecture notes in computer science*, vol. 2208. Utrecht: Springer; 2001. p. 249–58.
80. Korb W, Kornfeld M, Birkfellner W, et al. Risk analysis and safety assessment in surgical robotics: a case study on a biopsy robot. *Minim Invasive Ther Allied Technol.* 2005;14:23–31.
81. Larson AC, Wang D, Atassi B, et al. Transcatheter intraarterial perfusion: MR monitoring of chemoembolization for hepatocellular carcinoma—feasibility of initial clinical translation. *Radiology.* 2008;246:964–71.
82. Kim CK, Choi D, Lim HK, et al. Therapeutic response assessment of percutaneous radiofrequency ablation for hepatocellular carcinoma: utility of contrast-enhanced agent detection imaging. *Eur J Radiol.* 2005;56:66–73.
83. Leyendecker JR, Dodd 3rd GD, Half GA, et al. Sonographically observed echogenic response during intraoperative radiofrequency ablation of cirrhotic livers: pathologic correlation. *AJR Am J Roentgenol.* 2002;178:1147–51.
84. Permpongkosol S, Nielsen ME, Solomon SB. Percutaneous renal cryoablation. *Urology.* 2006;68:19–25.
85. Saksena M, Gervais D. Percutaneous renal tumor ablation. *Abdom Imaging.* 2009;34:582–7.
86. Hahn PF, Gazelle GS, Jiang DY, Compton CC, Goldberg SN, Mueller PR. Liver tumor ablation: real-time monitoring with dynamic CT. *Acad Radiol.* 1997;4:634–8.
87. Hamuro M, Kaminou T, Nakamura K, et al. Percutaneous ethanol injection under CT fluoroscopy for hypervascular hepatocellular carcinoma following transcatheter arterial embolization. *Hepatogastroenterology.* 2002;49:752–7.
88. Tsai H-M, Lin X-Z, Chen C-Y. Computed tomography demonstration of immediate and delayed complications of computed tomography-guided transthoracic percutaneous ethanol injection of hepatocellular carcinoma at the liver dome. [Miscellaneous Article].
89. Bao A, Goins B, Dodd 3rd GD, et al. Real-time iterative monitoring of radiofrequency ablation tumor therapy with 15O-water PET imaging. *J Nucl Med.* 2008;49:1723–9.
90. de Senneville BD, Mougnot C, Quesson B, Dragonu I, Grenier N, Moonen CT. MR thermometry for monitoring tumor ablation. *Eur Radiol.* 2007;17:2401–10.
91. Dewey WC. Arrhenius relationships from the molecule and cell to the clinic. *Int J Hyperthermia.* 1994;10:457–83.
92. Quesson B, de Zwart JA, Moonen CT. Magnetic resonance temperature imaging for guidance of thermotherapy. *J Magn Reson Imaging.* 2000;12:525–33.
93. Denis de Senneville B, Quesson B, Moonen CTW. Magnetic resonance temperature imaging. *Int J Hyperthermia.* 2005;21:515–31.
94. Rieke V, Butts Pauly K. MR thermometry. *J Magn Reson Imaging.* 2008;27:376–90.
95. Boss A, Rempp H, Martirosian P, et al. Wide-bore 1.5 Tesla MR imagers for guidance and monitoring of radiofrequency ablation of renal cell carcinoma: initial experience on feasibility. *Eur Radiol.* 2008;18:1449–55.
96. Liu HY, Hall WA, Martin AJ, Maxwell RE, Truwit CL. MR-guided and MR-monitored neurosurgical procedures at 1.5 T. *J Comput Assist Tomogr.* 2000;24:909–18.
97. Mack MG, Straub R, Eichler K, Sollner O, Lehnert T, Vogl TJ. Breast cancer metastases in liver: laser-induced interstitial thermotherapy—local tumor control rate and survival data. *Radiology.* 2004;233:400–9.
98. Morikawa S, Inubushi T, Kurumi Y, et al. MR-guided microwave thermocoagulation therapy of liver tumors: Initial clinical experiences using a 0.5 T open MR system. *J Magn Reson Imaging.* 2002;16:576–83.
99. Okuda S, Kuroda K, Oshio K, et al. MR-based temperature monitoring for hot saline injection therapy. *J Magn Reson Imaging.* 2000;12:330–8.

100. Seror O, Lepetit-Coiffe M, Le Bail B, et al. Real time monitoring of radiofrequency ablation based on MR thermometry and thermal dose in the pig liver in vivo. *Eur Radiol.* 2008;18:408–16.
101. Vogl TJ, Straub R, Eichler K, Sollner O, Mack MG. Colorectal carcinoma metastases in liver: laser-induced interstitial thermotherapy – local tumor control rate and survival data. *Radiology.* 2004;230:450–8.
102. Arthur RM, Straube WL, Trobaugh JW, Moros EG. Non-invasive estimation of hyperthermia temperatures with ultrasound. *Int J Hyperthermia.* 2005;21:589–600.
103. Fallone BG, Moran PR, Podgorsak EB. Noninvasive thermometry with a clinical x-ray CT scanner. *Med Phys.* 1982;9:715–21.
104. Efsthopoulos EP, Brountzos EN, Alexopoulou E, et al. Patient radiation exposure measurements during interventional procedures: a prospective study. *Health Phys.* 2006;91:36–40.
105. Stoeckelhuber BM, Leibecke T, Schulz E, et al. Radiation dose to the radiologist's hand during continuous CT fluoroscopy-guided interventions. *Cardiovasc Intervent Radiol.* 2005;28:589–94.
106. Gupta R, Grasmuck M, Suess C, et al. Ultra-high resolution flat-panel volume CT: fundamental principles, design architecture, and system characterization. *Eur Radiol.* 2006;16:1191–205.
107. Orth RC, Wallace MJ, Kuo MD. C-arm cone-beam CT: general principles and technical considerations for use in interventional radiology. *J Vasc Interv Radiol.* 2008;19:814–20.